

22

Normal Modes of a Compound Drop

M. Saffren, D. D. Elleman and W. K. Rhim

Jet Propulsion Laboratory
California Institute of Technology
4800 Oak Grove Drive
Pasadena, CA 91109

Abstract

In this paper we discuss a theory of normal modes of oscillation of compound liquid drops and the experiments performed to determine its validity. The modes are characterized by their frequency, the attendant displacement of fluid boundaries, and the flow pressure fields within the fluids. The drops consist of three fluids; a core fluid, a fluid shell surrounding the core, and a host fluid surrounding the shell. These fluids are assumed to be inviscid and incompressible, and the core and the shell to be concentric. The theory is obtained by linearization of the equations of fluid motion to the lowest order of nonlinearity that yields the normal modes. Numerical values of mode frequencies and the associated relative displacements of the fluid boundaries are presented for several specific systems, and the results compared with our observations. The core-centering phenomenon whereby the oscillations of the system tend to drive the shell and the core to be concentric was observed in the experiments and will be fully analyzed in a sequel.

Introduction

This is the first in a series of reports on the study of compound liquid drop systems. The systems consist of three fluids: a host fluid infinite in extent, that surrounds a second fluid in the form of a shell, which in turn surrounds a third fluid that forms the core. In particular we will investigate the several normal modes of compound drops on the assumptions: (i) the density of the fluids and the interfacial tensions are arbitrary, (ii) the fluids are incompressible, (iii) they are inviscid, (iv) the equations of fluid motion are linearized to the lowest order of nonlinearity that yields the class of normal modes being studied, and (v) the two fluid interfaces are nearly spherical and concentric. In ensuing reports we relax conditions (iii) through (v).

The primary aim of the entire study is to gain sufficient understanding of the behavior of compound drops to plan and interpret experiments in the laboratories, in the weightless environment provided by flight on the KC-135 aircraft and the Space Shuttle.

Aside from its interest as a fundamental study of compound drops, the work can be applied to the fabrication of fusion target pellets, development of containerless materials processing techniques both terrestrial and extra-terrestrial, and development of techniques for liquid drop control that can be used for fundamental studies in other scientific disciplines such as superfluid drop dynamics.

Equations of motion

We consider a system of several inviscid, incompressible fluids that are in contact with one another at the fluid boundaries each of which is characterized by an interfacial tension. The equations of motion for the system are well known and in spherical coordinates are given as:

v^2 psi = 0 (1)

dR/dt = (r-hat - v\_s R/R) . v psi (2)

sigma v\_s . n-hat = - delta [ rho d^2 psi/dt^2 + P - sigma (v psi)^2 ] (3)

The first equation for the velocity potential in each fluid follows from the assumption of incompressibility. The second equation is also kinematic and states that the fluid boundary moves with the fluids; the equation of a boundary being given as r = R(theta, phi, t). In eq. (2), r-hat denotes the unit vector along r, the vector from the origin to R(theta, phi), and v\_s denotes the surface gradient operator given by

ORIGINAL FACE IS  
OF POOR QUALITY

$$\bar{\nabla}_s = \hat{\theta} \frac{\partial}{\partial \theta} + \frac{\hat{\phi}}{\sin \theta} \frac{\partial}{\partial \phi} \quad (4)$$

Equation (3) is a dynamical equation indicating that the stress across an interface depends solely on its interfacial tension,  $\sigma$ . The left side of eq. (3) is the stress at a point on the boundary.  $\hat{n}$  is the surface normal at the point, and  $\bar{\nabla}_s$  denotes the surface divergence operator. The right side of this equation is simply the pressure difference supported by the boundary stress, and  $P$  denotes the pressure in the resting fluid.

These nonlinear equations are rendered linear by assuming that the motion of the system produces small deviations of a boundary from the shape it had when the system was at rest. For a compound drop the boundaries are spherical, and the pressure difference across a boundary of radius  $\bar{R}$  and interfacial tension,  $\sigma$ , is

$$\Delta P = - \frac{2\sigma}{\bar{R}}. \quad (5)$$

For this system, retaining only first order terms, eq. (2) can be written as

$$\frac{\partial R}{\partial t} - \frac{\partial \psi}{\partial r} = 0, \quad (2A)$$

and eq. (3) after substituting eq. (5), becomes

$$\Delta \left( \rho \frac{\partial \psi}{\partial t} \right) = \frac{\sigma}{\bar{R}^2} (2 - L^2) \Delta R, \quad (3A)$$

where  $\Delta R = R - \bar{R}$ , and  $L^2$  is the surface Laplacian which results from the linearization of the curvature.

Normal modes of a concentric three fluid systems

We consider a concentric three fluid system as shown in Figure 1, and calculate normal modes using eqs. (1), (2A), and (3A). The solution of the equations involves finding flow potential,  $\psi$ , in the three fluids. Since  $\psi$  is nonsecular solution of Laplace equation, it can be expressed in the following forms in each region of the system:

$$\psi(\underline{r}, t) = \sum_{\ell, m} [A(\ell, m; t)r^\ell + B(\ell, m; t)r^{-(\ell+1)}] Y_{\ell m}(\theta, \phi) \quad (\text{shell}) \quad (6)$$

$$\psi_i(r, t) = \sum_{\ell, m} A_i(\ell, m; t)r^\ell Y_{\ell m}(\theta, \phi), \quad (7) \quad (\text{core})$$

$$\psi_o(\underline{r}, t) = \sum_{\ell, m} B_o(\ell, m; t)r^{-(\ell+1)} Y_{\ell m}(\theta, \phi). \quad (8) \quad (\text{host})$$

If the condition that the normal component of velocity across each boundary is continuous is imposed, we obtain.

$$A_i = A - \frac{\ell + 1}{\ell} B R_i^{-(2\ell+1)} \quad (9)$$

$$B_o = B - \frac{\ell}{\ell + 1} \bar{R}_o^{(2\ell+1)} \quad (10)$$

Therefore, only the flow potential in the shell remains to be determined.

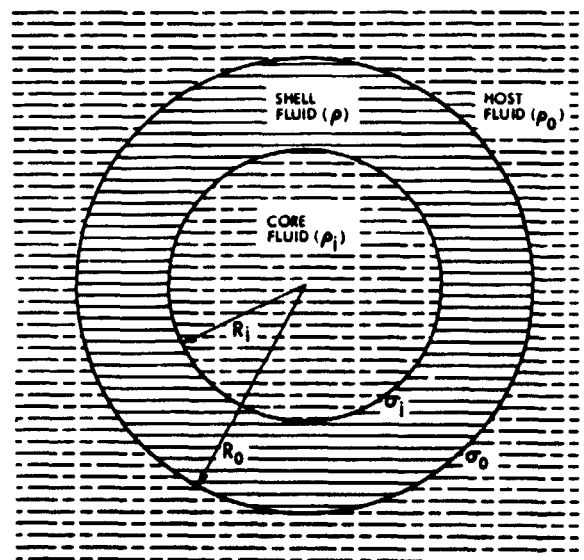


Figure 1. A concentric three fluid system used in the theory.

We now express the boundary functions in the following way:

$$R_{\begin{pmatrix} i \\ o \end{pmatrix}}(\theta, \phi; t) = \bar{R}_{\begin{pmatrix} i \\ o \end{pmatrix}} + \Delta R_{\begin{pmatrix} i \\ o \end{pmatrix}}(\theta, \phi; t) = \bar{R}_{\begin{pmatrix} i \\ o \end{pmatrix}} + \sum_{\ell, m} \delta R_{\begin{pmatrix} i \\ o \end{pmatrix}}(\ell, m; t) Y_{\ell m}(\theta, \phi). \quad (11)$$

If we substitute these expressions into eqs. (2A) and (3A), we show that the equations can be reduced to an eigenvalue equation which is essentially same as a coupled harmonic oscillator:

$$\begin{bmatrix} \frac{\sigma m_i}{\tau^3} & 1 \\ 1 & \frac{m_o \tau^3}{\sigma} \end{bmatrix} \begin{bmatrix} \Delta_o \\ \Delta_i \end{bmatrix} = -\frac{J}{W} \begin{bmatrix} \ddot{\Delta}_o \\ \ddot{\Delta}_i \end{bmatrix} \quad (12)$$

where

$$\sigma = \sqrt{\sigma_o/\sigma_i}, \quad \Delta_o \equiv \sqrt{\sigma} \delta R_o, \quad \Delta_i \equiv \delta R_i / \sqrt{\sigma}, \quad (13)$$

$$m_{\begin{pmatrix} o \\ i \end{pmatrix}} = (1 + \tilde{\Delta}_\rho \begin{pmatrix} o \\ i \end{pmatrix}) \tau^{(2\ell+1)} - \tilde{\Delta}_\rho \begin{pmatrix} o \\ i \end{pmatrix} \tau^{-(2\ell+1)}, \quad (14)$$

$$\tilde{\Delta}_\rho \begin{pmatrix} i \\ o \end{pmatrix} = \frac{(\ell+1)(\rho_i - \rho)}{(2\ell+1)\rho}, \quad \tilde{\Delta}_\rho \begin{pmatrix} o \\ o \end{pmatrix} = \frac{\ell(\rho_o - \rho)}{(2\ell+1)\rho} \quad (15)$$

$$J = (1 + \tilde{\Delta}_\rho \begin{pmatrix} o \\ o \end{pmatrix})(1 + \tilde{\Delta}_\rho \begin{pmatrix} i \\ i \end{pmatrix}) \tau^{(2\ell+1)} - \tilde{\Delta}_\rho \begin{pmatrix} i \\ i \end{pmatrix} \tilde{\Delta}_\rho \begin{pmatrix} o \\ o \end{pmatrix} \tau^{-(2\ell+1)}, \quad (16)$$

$$W = \left( \frac{\sigma_o \sigma_i}{[R_o R_i]^3} \right)^{1/2} \frac{(\ell-1)\ell(\ell+1)(\ell+2)}{(2\ell+1)\rho} \quad (17)$$

where  $\tau = \sqrt{R_o/R_i}$ . Note that the only dimensional quantity is  $W$  which has the dimension of frequency squared.

From eq. (12), the eigenvalues are given by

$$K = \frac{1}{2} \left( \frac{\sigma m_i}{\tau^3} + \frac{m_o \tau^3}{\sigma} \right) \pm \sqrt{\frac{1}{4} \left( \frac{\sigma m_i}{\tau^3} - \frac{m_o \tau^3}{\sigma} \right)^2 + 1}, \quad (18)$$

so that the normal mode frequencies  $\omega_{\pm}^2$ , are given by

$$\omega_{\pm}^2 = \frac{K}{J} W \quad (19)$$

From (11) and (17), we obtain the corresponding eigenvectors as

$$\frac{1}{\sigma} \begin{pmatrix} \delta R_o \\ \delta R_i \end{pmatrix}_{\pm} = \begin{pmatrix} \Delta_o \\ \Delta_i \end{pmatrix}_{\pm} = \frac{1}{d \pm \sqrt{d^2 + 1}} \quad (20)$$

where

$$d = \frac{1}{2} \left( \frac{m_o \tau^3}{\sigma} - \frac{\sigma m_i}{\tau^3} \right). \quad (21)$$

It follows from the orthogonality of eigenvectors that

$$\delta \left( \frac{\delta R_o}{\delta R_i} \right) = -\frac{1}{\sigma} \left( \frac{\delta R_o}{\delta R_i} \right)^{-1} \quad (22)$$

It is important to note that the positive square root in (20) corresponds to the positive square root in (18). Consequently for the normal mode with the higher frequency, the boundary oscillations are in-phase. We call this high frequency, "+", mode the "bubble" mode and the lower frequency, "-", mode the "sloshing" mode. From relation (22), the relative boundary displacement of the sloshing mode is out of phase. The relative boundary displacement of these two modes as they were observed in the neutral buoyancy tank is shown in Figure 2. The top figure shows "bubble" mode in which the two boundaries oscillate in-phase, and the bottom figure shows "sloshing" mode in which the two boundaries move out of phase. In this compound drop the core and the host were silicon oil, and the shell was water.

#### Velocity potential

We now obtain expressions of velocity potentials  $\psi_i$ ,  $\psi_s$  and  $\psi_o$  for the flow fields in the core, shell and the host respectively in terms of the interfacial displacements. From eqs. (6) through (11), the expressions for  $\psi_i$  and  $\psi_o$  are obtained as

$$\begin{aligned} (\psi_i)_{\ell m} &= \frac{s}{\tau} \tau^{\ell-1} \left( \frac{r}{s} \right)^{\ell} Y_{\ell m} \delta \dot{R}_i \\ (\psi_o)_{\ell m} &= -\frac{s}{\tau+1} \tau^{\ell+2} \left( \frac{s}{r} \right)^{\ell+1} Y_{\ell m} \delta \dot{R}_o \end{aligned} \quad (23)$$

where

$$s = \sqrt{\bar{R}_o \bar{R}_i} \quad \text{and} \quad \tau = \sqrt{\bar{R}_o / \bar{R}_i} \quad (24)$$

The result for  $\psi_s$ , interesting enough, can be expressed as

$$(\psi_s)_{\ell m} = (\psi_s^C)_{\ell m} + (\psi_s^H)_{\ell m} \quad (25)$$

where  $\psi_s^C$  is the shell velocity potential when the core is rigid and  $\psi_s^H$  is for the case when the host is rigid. When explicitly expressed, they are

$$(\psi_s^C)_{\ell m} = \frac{s_1^2}{(\ell+1)D} \left\{ (\ell+1) \tau^{\ell} \left( \frac{r}{s} \right)^{\ell} + \tau^{-(\ell+1)} \left( \frac{s}{r} \right)^{\ell+1} \right\} Y_{\ell m} \delta \dot{R}_o \quad (26)$$

$$(\psi_s^H)_{\ell m} = -\frac{s_1^{-2}}{\ell(\ell+1)D} \left\{ (\ell+1) \tau^{-\ell} \left( \frac{r}{s} \right) + \tau^{\ell+1} \left( \frac{s}{r} \right)^{\ell+1} \right\} Y_{\ell m} \delta \dot{R}_i \quad (27)$$

where  $D = \tau^{2\ell+1} - \tau^{-(2\ell+1)}$ . Of course, conditions

$$\left( \frac{\delta \psi_s^C}{\delta \dot{R}_o} \right)_{r=R_i} = 0 \quad \text{and} \quad \left( \frac{\delta \psi_s^H}{\delta \dot{R}_i} \right)_{r=R_o} = 0 \quad \text{were imposed to obtain (26) and (27).}$$

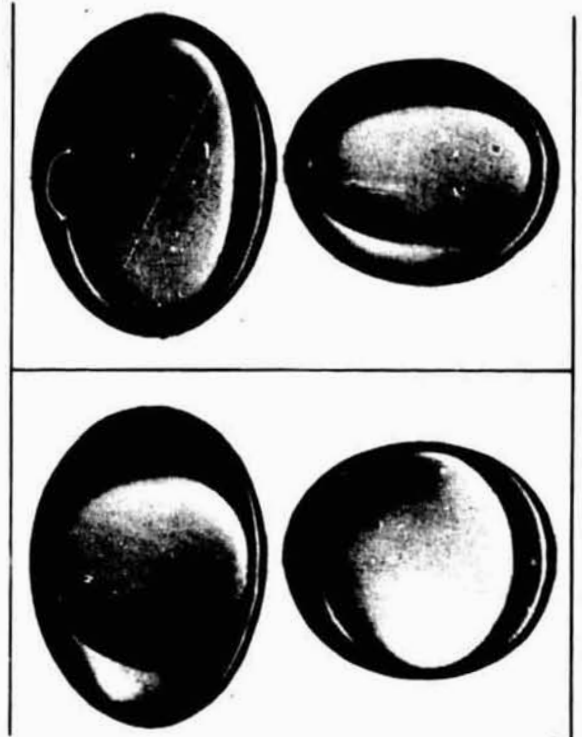


Figure 2. "Bubble" mode (top) and "sloshing" mode (bottom) oscillations of an oil-water compound drop.

Illustrative examples

Using eqs. (13) to (19), numerical values of the eigenfrequencies for various physical parameters can be readily obtained. Furthermore, simple expressions of several limiting cases as shown below can be deduced in a straightforward way.

(i) Simple Drop: We tested the present theory by deriving the well-known simple drop case. With  $R_1=0$  and following the procedure derived in the previous section, we get

$$\omega_L^2 = \frac{\epsilon(\epsilon+1)(\epsilon-1)(\epsilon+2)}{R^3 [\epsilon\rho_0 + (\epsilon+1)\rho]} \quad (28)$$

which is identical to Lamb's result.<sup>2</sup> Figure 3 shows various modes of a simple drop corresponding to the different values of  $\epsilon$ . A water drop immersed in a neutrally buoyant oil bath was axisymmetrically excited by a plunger which was in turn connected to a sinusoidally excited loud speaker. With 1.5cc of drop volume, the interfacial tension, 11.2 dynes/cm, was obtained using eq. (28) for  $\epsilon = 2$ . The higher mode frequencies obtained using eq. (28) is shown in Figure 4 (solid line) and it was compared with the actual measurements (circles). The agreement is excellent.

(ii) Rigid Host: When the compound drop was formed in the rigid host (i.e.,  $\rho_0 = \infty$ ), then  $\omega_- = 0$  and

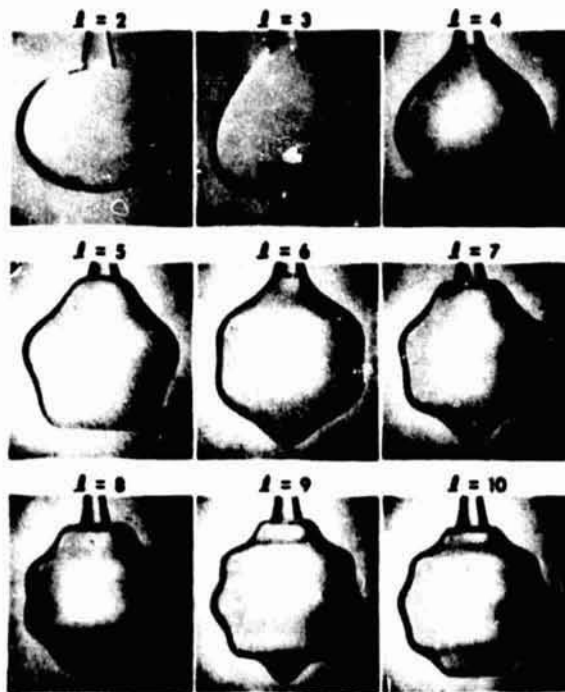


Figure 3. Various modes of a water drop oscillations in the silicon oil bath. The drop was mechanically excited.

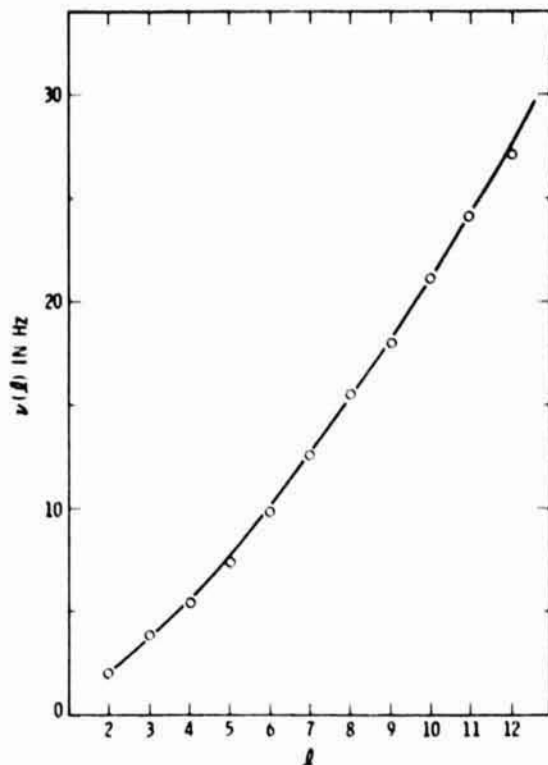


Figure 4. Frequency vs  $\epsilon$  of a water drop in silicon oil. Drop volume was 1.5cc, and  $\sigma = 11.2$  dynes/cm as measured for  $\epsilon = 2$  case. Under these conditions, the solid line was obtained using eq. (28), and the circles were as measured by the mechanically excited oscillations.

$$\omega_{\pm}^2 = \frac{\rho_1(\epsilon-1)\epsilon(\epsilon+1)(\epsilon+2)[\epsilon^{2\epsilon+1} - \epsilon^{-(2\epsilon+1)}]}{R_1^3 \{ [\epsilon\rho_0 + (\epsilon+1)\rho_1] \epsilon^{2\epsilon+1} + (\epsilon+1)(\rho - \rho_1) \epsilon^{-(2\epsilon+1)} \}} \quad (29)$$

If we normalize this with respect to  $\omega_L$  of a simple drop which is made out of shell fluid immersed in the core fluid, then  $N_0 = \omega_{\pm} / \omega_L$  for  $\epsilon=2$  and  $\rho_1 = \rho$  is as shown in Figure 5. Here  $V_T$  is the total volume (i.e.,  $V_T = V_{\text{shell}} + V_{\text{core}}$ ).  $N_0$  rises from zero at  $V_T/V_C = 1$ , then it approaches to infinity as the core shrinks. As the core shrinks with respect to  $V_T$ , the core motion becomes essentially decoupled from the host and approaches to the simple drop frequency. This can be readily observed from eq. (29) as

$$N_0 = \sqrt{\epsilon / R_1} \rightarrow \infty$$

(iii) Rigid Core: If the compound drop has rigid core (i.e.,  $\rho_1 = \infty$ ), then  $\omega_- \rightarrow 0$ , and

$$\omega_+^2 = \frac{\rho_0(\epsilon-1)\epsilon(\epsilon+1)(\epsilon+2)[\epsilon^{2\epsilon+1} - \epsilon^{-(2\epsilon+1)}]}{R_0^3 \{ [\epsilon\rho_0 + (\epsilon+1)\rho_1] \epsilon^{2\epsilon+1} + \epsilon(\rho - \rho_0) \epsilon^{-(2\epsilon+1)} \}} \quad (30)$$

Of course, when  $R_1 \rightarrow 0$ , this reduces to eq. (28) for the simple drop. If we let  $\omega_L$  be this simple drop frequency, then the normalized frequency,  $N_c = \omega / \omega_L$ , for  $l=2$  and  $\rho_0 = \rho$ , is as shown in Figure 6. Starting from a very thin shell (i.e.,  $V_T/V_C = 1$ ),  $N_c$  rises sharply to its maximum, then gradually approaches the single drop frequency as  $V_T/V_C$  increases. The agreement with the experimental points is fairly good.

(iv) Thin Shell: When the shell is very thin (i.e.,  $\tau = 1$ ), then  $\omega_- = 0$ , and

$$\omega_+^2 = \frac{(\sigma_0 + \sigma_1)(l-1)l(l+1)(l+2)}{R^3 [l\rho_0 + (l+1)\rho_1]} \quad (31)$$

Note that this is the same expression as that of a simple drop if its interfacial surface tension is replaced by  $\sigma_0 + \sigma_1$ . This particular result was also confirmed experimentally in the neutral buoyancy tank

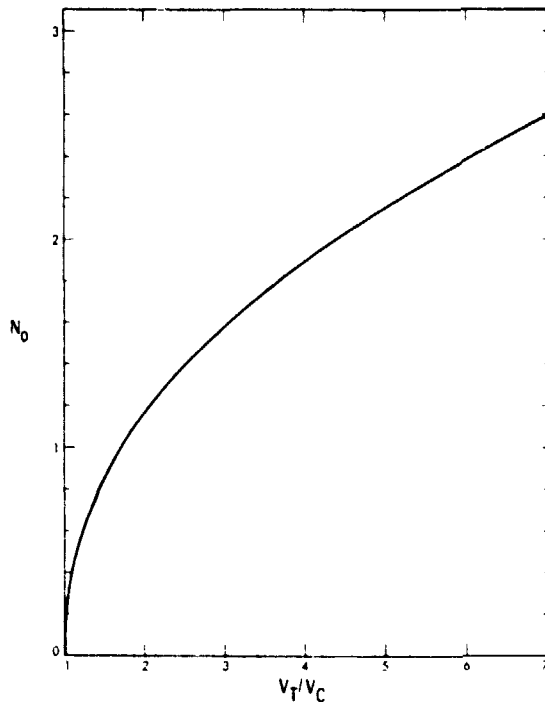


Figure 5. Normalized Frequency,  $N_0$  vs  $V_T/V_C$  when the hose is rigid.

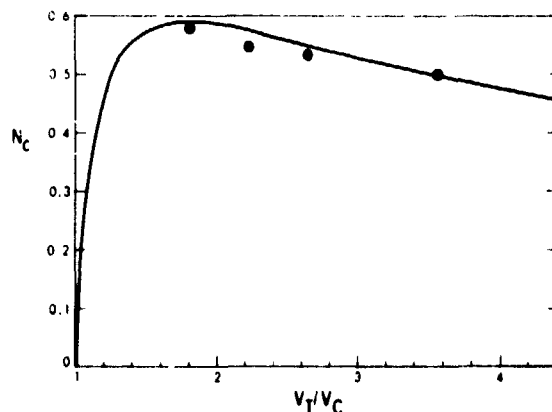


Figure 6. Normalized frequency,  $N_c$ , vs  $V_T/V_C$  when the core is rigid.

(v) Thick Shell: When the shell is very thick (i.e.,  $\tau \rightarrow \infty$ ), then we get

$$\omega_+^2 \rightarrow \frac{4\pi\sigma_1(l-1)l(l+1)(l+2)}{3V_C [l\rho + (l+1)\rho_1]} \quad (32)$$

and

$$\omega_-^2 \rightarrow \frac{4\pi\sigma_0(l-1)l(l+1)(l+2)}{3V_S [l\rho_0 + (l+1)\rho]} \quad (33)$$

where  $V_C$  and  $V_S$  are the core and the shell volumes respectively. These expressions tell us that in this limit the "bubble" and "sloshing" modes are no longer coupled since each mode represents simple drop oscillation.

(vi) For  $\rho_1 = \rho_0$  and  $\sigma_1 = \sigma_0$ : When the core and the host fluids are the same and the two interfacial tensions are the same the expressions for  $\omega_{\pm}^2$  cannot be made much simpler than eq. (19). However, the numerical results of these frequencies are shown in Figure 7, where  $V_T = V_C + V_S$ , and  $N_s = \omega_{\pm} / \omega_L$  where  $\omega_L$  is the frequency of a simple drop which is made out of the same compound drop when the core was reduced to zero. In this figure the upper five curves represent "bubble" modes for the specified values of  $\rho_1/\rho$  when  $\rho_1 = \rho_0$ , and the lower three curves represent corresponding "sloshing" modes. Experimental points taken in a neutral buoyancy tank ( $\rho_1/\rho = \rho_0/\rho = 1$ ) show good agreement with the theoretical curves. The results for the relative boundary displacements are shown in Figure 8 for an air-water-air type and an oil-water-oil type of compound drop systems. We see that our preliminary experimental results obtained in a neutral buoyancy tank also agree well with the theory.

#### Remarks on core centering

An interesting core centering phenomenon was observed in our neutral buoyancy experiments. Initially, a static compound drop was prepared so that the inner and the outer boundary surfaces were nonconcentric due to the slight density mismatch. However, as the drop began to oscillate in one of its normal mode frequencies (for  $l=2$ ), the two boundaries became concentric within the accuracy of our observation. Though this

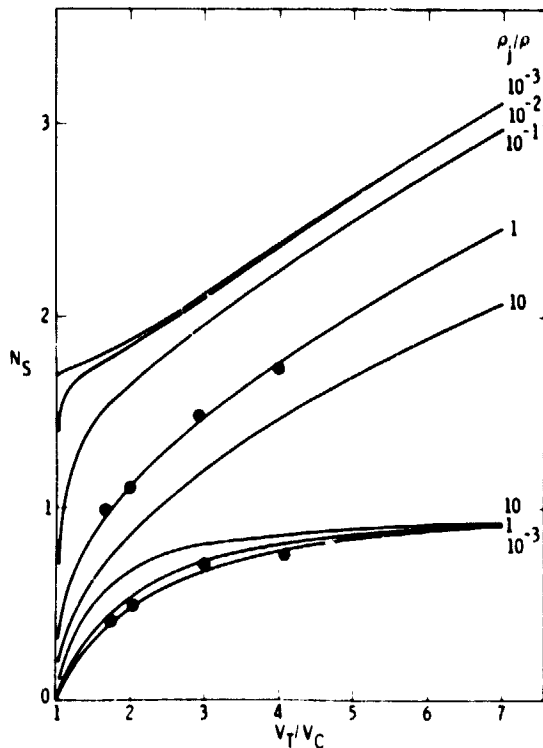


Figure 7. Normalized frequency,  $N_s$ , vs  $V_T/V_C$  when  $\sigma_1 = \sigma_0$  and  $\sigma_1 = \sigma_0$ . The upper five curves are for the "bubble" modes and the lower three curves are for the "Sloshing" modes.

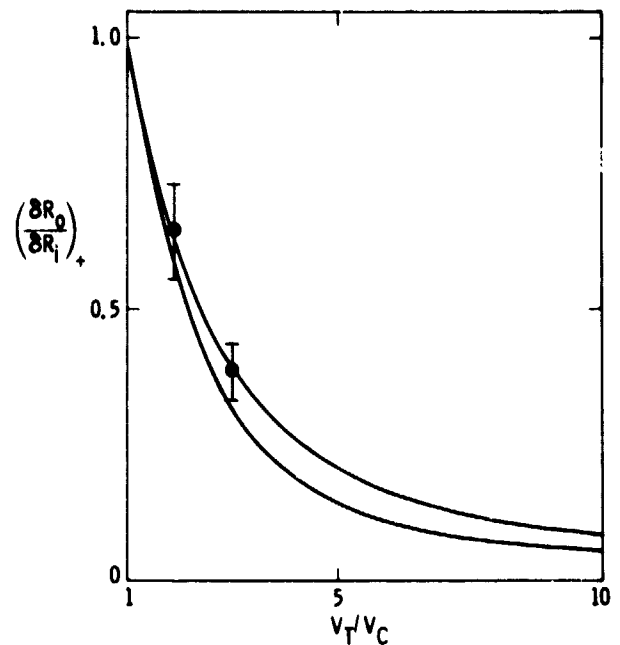


Figure 8. Relative boundary displacement of "bubble" modes. The upper curve is for an oil-water-oil type of compound drop and the lower curve is for an air-water-air type of compound drop. The experimental points are from the neutral buoyancy experiment.

centering phenomenon takes place within a few cycles of oscillation, the centering force seems to depend, among others, on the oscillation amplitude and the shell thickness. Within the approximations used in this paper, the positions of the core anywhere within the drop is neutrally stable. It is necessary to consider the next order of approximation to find the restoring forces responsible for the centering of the core and the shell. Work on the centering phenomenon and its more detailed description will be published elsewhere.

#### Experimental apparatus and procedure

(A) Neutral Buoyancy Tank: The heart of the experimental apparatus is a neutral buoyancy tank which is a lucite box filled with silicon oil (Dow Corning 200, lcs). Taking advantage of the fact that the density of silicon oil was less than water, we created a vertical density gradient by adding a small amount of freon to the silicon oil until the water droplet floated in the middle of the tank. Also imbedded within this box were several electrodes for the purpose of excitation and detection of the drop systems.

(B) Excitation and Detection Procedure: We adopted basically two different detection procedures: 1) frequency sweep, and 2) the pulsed transient technique. In the continuously driving method, the frequency of an oscillating electric field was swept through resonances while monitoring the oscillation amplitude using an optical recording and video systems (such as fast movie camera or TV video system). This method has the advantage of quick identification of the characteristic oscillations and provides detailed information about boundary motion. However, it was found that unless the driving field was kept at a low level, the resonance frequency measured in this method was erroneous. This is due to the fact that the large oscillating electric field changes the surface tension dynamically. The detection method which was used extensively in this experiment was the capacitance bridge method. The block diagram of this apparatus is shown in Figure 9. This method is similar in principle to more well-known transient techniques in nuclear magnetic resonance or optical spectroscopy. The basic idea of this technique is to record capacitance variation as the drop evolves freely toward equilibrium state from an initial nonequilibrium state. Application of an intense short electric pulse excites the droplet over a wide range of frequency simultaneously. Therefore, the Fourier transformation of this transient signal reveals characteristic frequencies simultaneously.

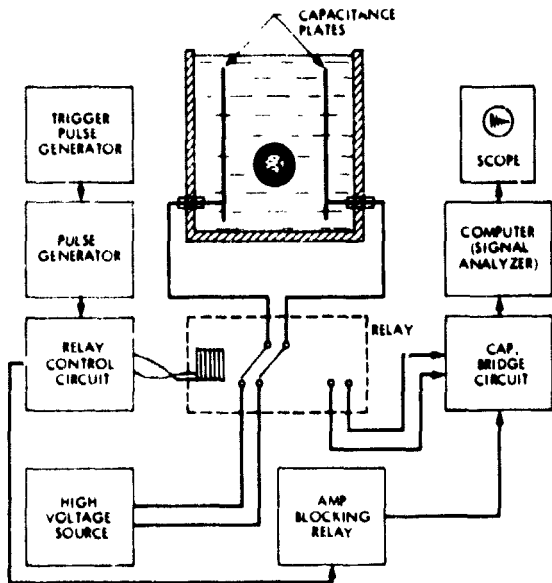


Figure 9. A block diagram of our apparatus which excites the drop electro-statically and detects the ensuing capacitance signal caused by the drop deformation.

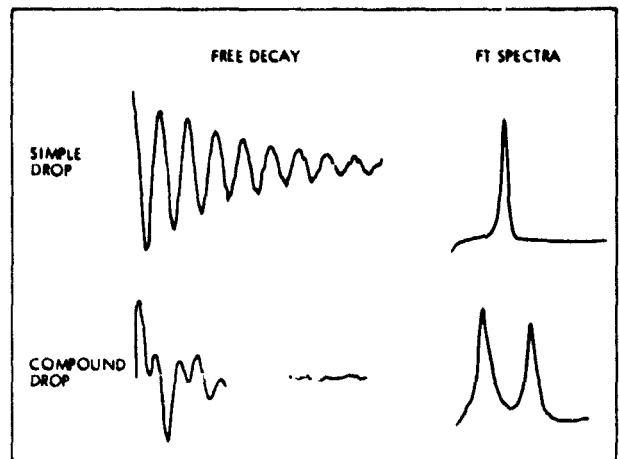


Figure 10. Signals obtained by the capacitance bridge and their Fourier transformed spectra.

This capacitance bridge system was constructed around a General Radio Capacitance Bridge Unit, a home-built relay system, an A/D converter, and a data processing minicomputer. Once the capacitance bridge was balanced with the relay connected to the bridge, an electric pulse could be fired by simply controlling the relay switch for the preset time duration. Upon the termination of the pulse, the electrodes were switched back to the bridge and the ensuing signal was detected and processed. In order to protect the amplifier during the pulse and to shorten the recovery time following the pulse, an amplifier blocking relay switch was inserted at the input of the amplifier.

Figure 10 shows a set of typical data obtained in this method. For the simple drop case, the signal is a damped monotonic oscillation which corresponds to a single peak in the frequency domain. Of course, the spectral line width is inversely proportional to the damping time constant of the time domain signal. The signal from a compound drop looks more complicated. However, Fourier transformation shows two well-resolved peaks each of which corresponds to the bubble mode and the slushing mode respectively. Though the capacitance bridge method provides a full spectrum without scanning through resonance frequencies, it does not provide information about boundary motion. For this reason it is more convenient to adopt both continuous and transient methods which will compliment each other.

#### Acknowledgement

The authors express their deep and warm appreciation to Dr. John Carruthers without whose interest, encouragement, and support this work would not have been possible. The authors also would like to extend their appreciation to J. Shanks and A. Croonquist for their assistance.

#### References

1. Landaw, L. D., and Lifshitz, E. M., Fluid Mechanics, (Pergamon Press, London), pp. 239.
2. Lamb, H., Hydrodynamics, Sixth Edition, Cambridge University Press, Reprinted by Dover, New York, 1945, pp. 475.